UNIVERSITY OF LEEDS

Article:
Wolter, M, de Vink, P, Neves, JF et al. (7 more authors) (2020) Selectivity via Cooperativity: Preferential Stabilization of the p65/14-3-3 Interaction with Semisynthetic Natural Products. Journal of the American Chemical Society, 142 (27). pp. 11772-11783. ISSN 0002-7863

https://doi.org/10.1021/jacs.0c02151

Selectivity via Cooperativity: Preferential Stabilization of the p65/14-3-3 interaction with Semi-Synthetic Natural Products.

Madita Wolter[1], Pim de Vink[1], João Filipe Neves[2,3], Sonja Srdanović[4], Yusuke Higuchi[5], Nobuo Kato[5], Andrew Wilson[4,6], Isabelle Landrieu[2,3], Luc Brunsveld[1], Christian Ottmann[1]*.

1 Laboratory of Chemical Biology, Department of Biomedical Engineering and Institute for Complex Molecular Systems, Technische Universiteit Eindhoven, P.O. Box 513, Eindhoven 5600 MB , The Netherlands.

2 Univ. Lille, Inserm, CHU Lille, Institut Pasteur de Lille, U1167 - RID-AGE - Risk Factors and Molecular Determinants of Aging-Related Diseases, F-59000 Lille, France

3 CNRS ERL9002 Integrative Structural Biology F-59000 Lille, France

4 School of Chemistry, University of Leeds, Woodhouse Lane, Leeds, LS2 9JT, UK

5 The Institute of Scientific and Industrial Research, Osaka University, Ibaraki, Osaka 567-0047, Japan

6 Astbury Centre for Structural Molecular Biology, University of Leeds, Woodhouse Lane, Leeds, LS2 9JT, UK

Keywords: Protein-protein interactions, stabilization, cooperativity, NF-κB, natural products, RelA

ABSTRACT: Natural compounds are an important class of potent drug molecules including some retrospectively found to act as stabilizers of protein-protein interactions (PPIs). However, the design of synthetic PPI stabilizers remains a poorly investigated approach. To this date, there are no general procedures available to evaluate the induced cooperativity of the interacting proteins due to the stabilizer molecule. The 14-3-3 scaffold proteins provide an excellent platform to explore PPI stabilization because these proteins mediate several hundred PPIs, and a class of natural compounds – the fusicoccanes – are known to stabilize a number of 14-3-3 protein interactions. 14-3-3 has been reported to negatively regulate the p65 subunit of the NF-κB transcription factor, qualifying this protein complex as a potential target for drug discovery in order to control cell proliferation. Here, we report the high-resolution crystal structures of two 14-3-3 binding motifs of p65 in complex with 14-3-3. A semi-synthetic natural product derivative – DP-005 – binds to an interface pocket of the p65/14-3-3 complex and concomitantly stabilizes it. Cooperativity analyses of this interaction, and other disease relevant 14-3-3-PPIs, demonstrated selectivity of DP-005 for the p65/14-3-3 complex. The adaptation of a cooperative binding model provided furthermore a general approach to characterize stabilization and to assay for selectivity of PPI stabilizers.

INTRODUCTION

The need to develop new strategies that address the challenges of today's most important diseases, has motivated efforts to modulate protein-protein interactions (PPIs), which has become an increasingly attractive approach for drug discovery.[1–4] Promising progress has been made on both inhibition and stabilization of PPIs, but especially the *ab initio* design of PPI stabilizers is still the exception.[3] Nature itself provides the most potent and selective stabilizers of PPIs, validating the concept of stabilization as a valuable strategy for targeting PPIs.[5,6] The mode of action of known PPI stabilizers was mostly discovered retrospectively, as for example with rapamycin (Rapamune®, Pfizer), cyclosporin (Sandimmun®, Novartis Pharmaceuticals) or FK506 (Prograf®, Astellas Pharma). [5–7]

In order to achieve PPI stabilization, the binding equilibrium of two target proteins needs to be shifted to the complexed state by binding of a third interaction partner, preferably a drug-like small molecule. This underlying binding improvement can be described via cooperative binding models whereby the increased binding affinity of the interaction partners, due to the formation of a ternary complex, is quantified via the cooperativity factor α.[8–11] Adapting the cooperativity model to PPI drug discovery projects has been an underexplored opportunity which has however started to gain more attention since PROTACs (proteolysis-targeting chimeras) were shown to induce cooperative binding of their protein binding partners.[12] In this work, using the interactions of 14-3-3 proteins as an example, we show that cooperativity analysis not only provides a description of binding properties but can also be used as a direct entry to establishing selectivity of compounds stabilizing PPIs. The 14-3-3 family of proteins pertain to the adaptor proteins which represent one of the most important protein classes in the PPI field, since they mediate interactions between proteins and

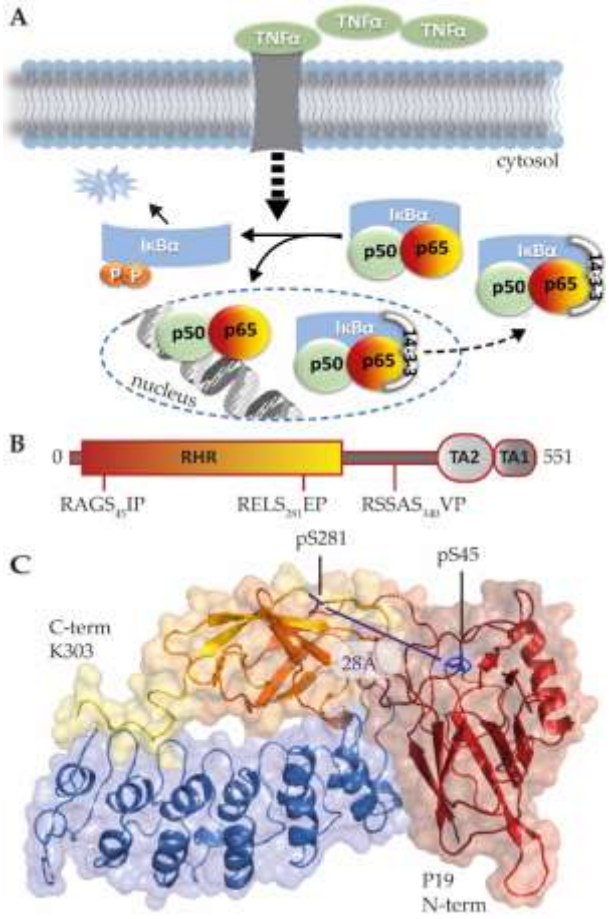

Figure 1: Interaction of p65 and 14-3-3. (A) Schematic representation of the interaction of 14-3-3, p65 and IκBα in context of the NF-κB pathway. Briefly, upon activation of the pathway (for example by TNFα) a signal cascade (represented by a thick dashed arrow) leads to the phosphorylation and degradation of IκBα and the nuclear translocation of NF-κB (here represented by p50/p65). Binding of IκBα and 14-3-3 to p65 are necessary for nuclear export or cytosolic retention (narrow dashed arrow). (B) Domain representation of the p65 protein, with the Rel Homology Region (RHR), the two transactivator domains (TA1, TA2) and amino acid sequences of the three conserved potential 14-3-3 binding sites. (C) Cartoon representation of the crystal structure of the complex of IκBα with RHR domain of p65, with Van der Waals' transparent surface. p65 (red to yellow) with IκBα (blue) (PDB ID: 1IKN; p50 hidden for clarity; S45 and S281 are highlighted for clarity).

thereby regulate the function of their partner proteins.[13,14] The 14-3-3 proteins recognize and bind phosphoserine/threonine motifs of hundreds of protein partners in eukaryotic cells, subsequently altering the catalytic activity, subcellular localization, or interactional preference of their partners.[15,16] 14-3-3 is functionally present as a w-shaped dimer featuring two highly conserved, amphipathic grooves, where the phosphorylated residues are bound.[17] A key element for the promising development of 14-3-3 proteins as potential drug targets is the availability of multiple members of a class of natural products - the fusicoccanes (FCs) – that have been demonstrated to stabilize the binding of 14-3-3 proteins to a number of partner proteins.[18–22] Protein crystallography studies have shown for example how such FCs stabilize 14-3-3 binding to protein targets like p53,[18] c-Raf,[19] ERα,[20] Gab2[21] and CFTR.[22] These natural compounds

bind to protein pockets delineated by the interface of the complex of 14-3-3 and its partner protein. In this way, FCs establish contacts to both protein partners simultaneously, acting as a molecular glue.[5,23]

Among the 14-3-3 partners are at least two proteins that crucially participate in the NF-κB pathway.[24–26] The NF-κB signaling pathway has raised considerable attention as a therapeutic target, because of its intimate involvement in cell proliferation, apoptosis, immunity, and inflammation via the expression of several hundred genes.[27–29] NF-κB proteins are dimeric transcription factors which are sequestered out of the nucleus into the cytosol by inhibitor proteins. Upon activation of the NF-κB pathway, for example by TNFα, NF-κB translocates to the nucleus and activates transcription (Figure 1A). Inhibition of this transcriptional activity has been the goal of numerous drug discovery campaigns, however only a limited number of inhibitors of the NF-κB pathway are currently marketed drugs, none of which directly target NF-κB.[30–32] The NF-κB subunit p65 and its inhibitor IκBα bind to 14-3-3, which favors localization of p65 in the cytosol.[24] Only limited information about the p65/14-3-3 interaction is available, even though downregulation of 14-3-3 leads to increased transcriptional activity of p65 in both, a breast cancer model[25] and studies on Ischemia-Reperfusion.[26] Stabilization of the p65/14-3-3 complex might therefore inhibit the transcriptional activity of p65, opening a new and unique opportunity for p65-specific NF-κB inhibition.

In this study we provide the structural and biophysical data and analysis to substantiate the biological interaction studies of the p65/14-3-3 interaction. We tested several natural and semi-synthetic FCs as potential small molecule stabilizers of this intriguing PPI, revealing the semi-synthetic DP-005 as the most active compound. A detailed analysis of the cooperative binding of the FCs, and DP-005 in particular, to the p65/14-3-3 interaction and multiple other disease relevant 14-3-3 PPIs was performed. DP-005 was at least 10-fold more active in stabilizing the p65/14-3-3 interaction than any other tested combination of FC and 14-3-3 PPI. The analysis clearly demonstrates that the cooperativity factor α can be used to quantify these stabilizing effects and is an underlying factor in achieving selectivity of stabilizer molecules on PPIs.

RESULTS AND DISCUSSION

Interaction of p65 and 14-3-3. In p65, the sequence surrounding three serines – S45, S281, S340 – matches to 14-3-3 consensus binding motifs (Figure 1B).[17] Mutations of these serine residues to alanines was previously shown to reduce p65 binding to 14-3-3 in cells and to increase the p65 concentration in the nucleus.[24] The S45 and S281 sites are phosphorylated in response to TNFα treatment[33] and both are

highly conserved within mammals (Figure S1). No TNFα dependent phosphorylation has been reported for the S340 site,[33] which is also less conserved (Figure S1). The pS45 and pS281 sites are located in unstructured loop regions of p65 and the folding of p65 brings these two residues into proximity with each other, implying the possibility for a bivalent interaction with the 14-3-3 dimer (Figure 1C).[22,34,35]

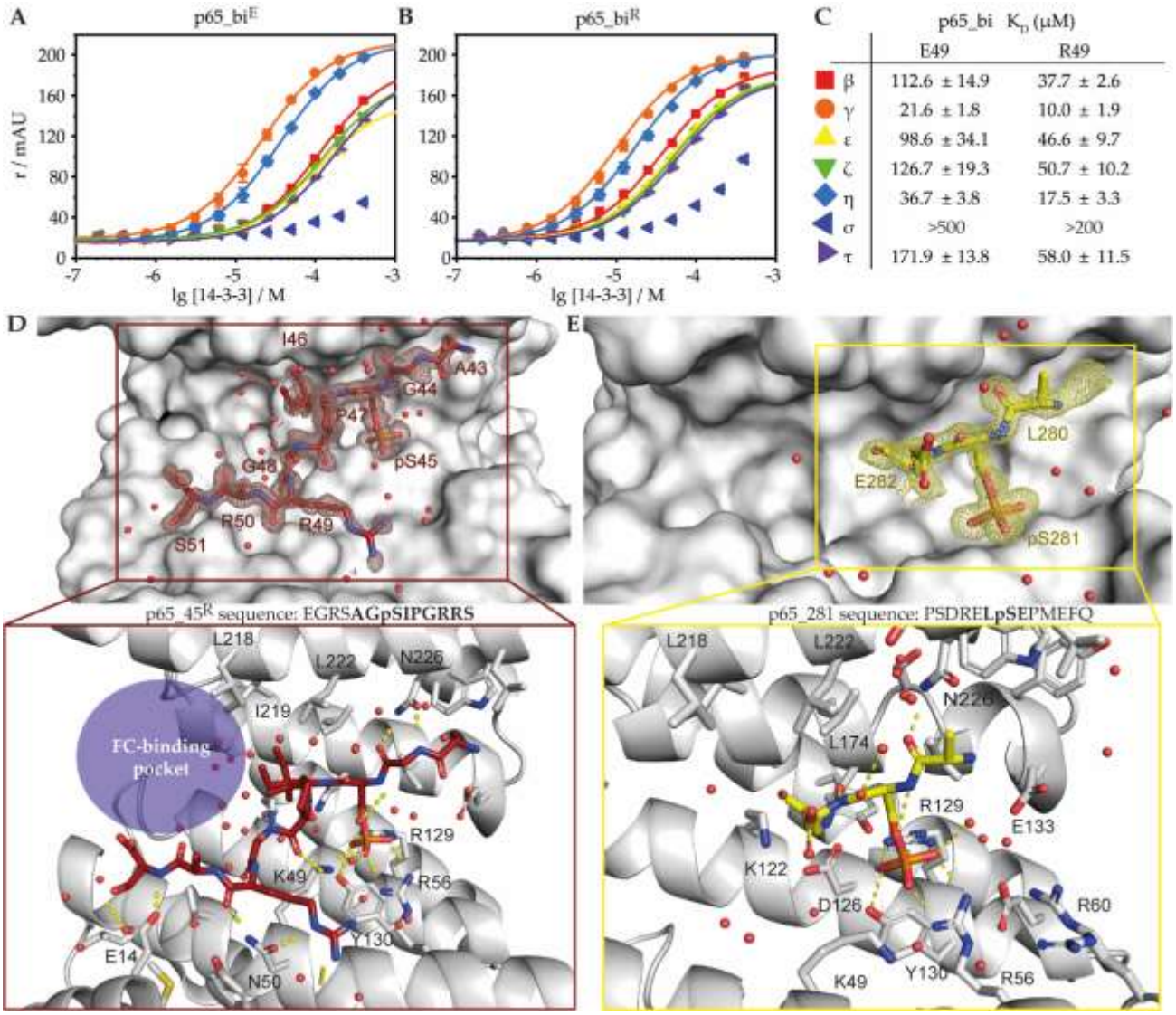

Figure 2: The binary complex of p65 peptides and 14-3-3. (A,B) The binding affinities of the indicated bivalent p65 peptides (100nM) to all human 14-3-3 isoforms were measured via fluorescence anisotropy (r in mAU) assays. (C) K_D values in µM of the p65_bi^E and p65_bi^R to the different 14-3-3 isoforms. (D) High resolution X-ray crystal structures of p65_45^R (PDB ID: 6QHL). The peptide shows a C-terminal curved conformation leaving the typical FC binding pocket more or less accessible (blue circle). (E) High resolution X-ray crystal structures of p65_281 (PDB ID: 6QHM) in complex with 14-3-3σΔC. The proteins are either displayed as white surface or cartoon (close up); water molecules are shown as red spheres. The 2mFo-Fc electron density map is displayed with σ=1. Polar contacts between protein and peptides are indicated as yellow dashed lines. Sequence of the p65_45^R peptide: EGRS**AGpSIPGRRS**; sequence of the p65_281 peptide: PSDRE**LpSE**PMEFQ (residues visible in the electron density are bold).

In order to represent these interaction motifs, peptides of 13 amino acids were synthesized for the pS45 and pS281 site (Table 1). Noteworthy, for the pS45 site two different sequences are available: whereas the canonical sequence features a glutamate at position 49, a second sequence identified an arginine instead.[36] Since no biological or phenotypic relevance of these variants are reported,[36] both sequences were tested for binding, hereafter termed p65_45^{E} and p65_45^{R} after the phosphorylation site S45 and the variant of amino acid 49. Each peptide is centered around the phosphorylated serine, flanked by six amino acids of the wildtype sequence on each side. To mimic the expected bivalent binding mode of the p65/14-3-3 complex double phosphorylated peptides were synthesized, connecting the two binding sites with a flexible linker (Table 1).

Elaboration of 14-3-3 binding motifs of p65. In a first step, the binding affinities of the two conserved 14-3-3 binding motifs of p65 were measured. To this end, the p65-peptides were labeled with a fluorophore and fluorescence anisotropy assays (FA) were performed. Both single site binding epitopes showed an increase in FA upon addition of 14-3-3 proteins, although not with full binding saturation (Figure S2). This confirms weak binding of both sites to all human 14-3-3 isoforms. The bivalent peptides featured a significantly stronger binding affinity to all 14-3-3 isoforms, with the p65_bi^{R} binding roughly 2-fold stronger than the p65_bi^{E} peptide (Figure 2A-C). The strongest binding was observed with 14-3-3γ (K_D^{E49}=21.6±1.8 μM; K_D^{R49} = 10.0±1.9 μM), directly followed by 14-3-3η (K_D^{E49}=36.7±3.8 μM; K_D^{R49}=17.5±3.3 μM), The dissociation constants of 14-3-3β, ε, ζ, and τ with p65_bi^{R} ranged from 38 to 127 μM (Figure 2C), while 14-3-3σ showed the weakest binding (Figure 2C), not atypical for 14-3-3.[22,37,38] The peptide-protein binding data thus confirm a physical interaction between p65 and 14-3-3 and argue in favor of a bivalent binding event.

The binding between p65 and 14-3-3 was further elucidated with structural data; the single phosphorylated peptides were co-crystallized with 14-3-3σΔC (last 17 unstructured residues on the C-terminus are truncated) resulting in high resolution structures of 1.2 and 1.25 Å for the p65_45^{R}, and p65_281 complexes, respectively (Table S1). The phosphorylated S45 makes polar contacts with R56, R129 and Y130; the general phospho-accepting pocket of 14-3-3 (Figure 2D; PDB-ID: 6QHL). Upstream of pS45 only A43 and G44 are visible in the electron density map, whereby the backbone of G44 makes polar contacts with N226 of the 14-3-3 protein. At the +1 position of pS45 the isoleucine points into a hydrophobic pocket of the 14-3-3 binding groove making hydrophobic contacts with L174, I219, and L222. The presence of a proline residue at the +2 position results in a curved conformation in the binding groove, potentially creating a ligandable interface pocket (Figure 2D). In comparable crystal structures of 14-3-3 with other

interaction partners, a similar pocket accommodates FCs and their derivatives.[18,19,21] The sidechain of R49 makes two polar contacts with N50 of 14-3-3 as well as with several water molecules. The C-terminus of the p65_45^{R} peptide makes additional polar contacts with E14 of 14-3-3. The direct comparison of the two variants of the p65_45 peptide only shows small differences in binding affinity and structural information could only be obtained for the p65_45^{R} peptide, hence this variant was selected for the next experiments.

Table 1: Overview of synthetic peptides representing the proposed 14-3-3 binding motifs of p65.

Name	Phospho-site	Peptide Sequence
p65_45^{E}	pS45	EGRSAGpS$_{45}$IPGE$_{49}$RS
p65_45^{R}	pS45	EGRSAGpS$_{45}$IPGR$_{49}$RS
p65_281	pS281	PSDRELpS$_{281}$EPMEFQ
p65_bi^{E}	pS45pS281	EGRSAGpS$_{45}$IPGE$_{49}$RSGSGGGSG PSDRELpS$_{281}$EPMEFQ
p65_bi^{R}	pS45pS281	EGRSAGpS$_{45}$IPGR$_{49}$RSGSGGGSG PSDRELpS$_{281}$EPMEFQ

The electron density of the p65_281 peptide in complex with 14-3-3 revealed only the backbone of two additional amino acids besides that of the phosphorylated serine (Figure 2E; PDB ID: 6QHM). Additional electron density on the N-terminus of the peptide could not be fully interpreted, indicating multiple conformations of these amino acids. The phosphoserine is trapped in the binding groove via polar contacts with R59, R129 and Y130 of 14-3-3σΔC. Additionally, contacts could also be observed with the backbone nitrogen of E282, at the +1 position of p65_281, and N175 of 14-3-3 and the carbonyl of L280 of the peptide and N226 of the protein.

Fusicoccanes stabilize the p65/14-3-3 interaction. The structures of p65_45^{R} and p65_281 provide the structural basis to investigate possible molecular strategies to stabilize these binary complexes. Since the 14-3-3 binding groove is highly conserved, the p65-peptide/14-3-3σΔC interface displays the key molecular details of the primary p65/14-3-3 interface.[17] The p65_45^{R} peptide is bending in a way that the typical FC binding pocket remains accessible and the conformation of the p65_281 is unknown (Figure 2D,E).

This leaves the possibility that both complexes may be stabilized by FCs or synthetic derivatives thereof. The FCs share a diterpene core with a 5(A)-8(B)-5(C) ring structure (Figure 3A);[39] modifications that include additional sugar moieties, hydroxylation or acetylation have introduced considerable chemical diversity into this compound family (Figure 3B).[40]

The effect of FCs on the p65/14-3-3 complex was investigated with a small collection of eight natural FCs and their semi-synthetic derivatives (Figure 3B). The tested FCs have a FC-A like structure with a hydroxylation on position 8, a methoxy group at position 16 and a sugar moiety at position 9. The main variations within the collection used here are on the sugar moiety, position 12, and/or 19. FC-A contains an additional acetyl on the 19 position, while the natural product FC-J only has an isopropyl on the C-ring. A recent study showed that replacing the acetyl with an acetamide (FC-NAc) improves the affinity to 14-3-3 with various partners.[23] The 12-position is hydroxylated in the natural compounds, but this position is not hydroxylated in the semi-synthetic derivatives DP-005 and ISIR-005[21,41] and a bulky group was introduced for FC-THF.[42] For FC-A-aglycon (FC-A-ag)[42] and FC-J-aglycon (FC-J-ag)[42] the sugar moiety was removed. Initially, a single-dose of compound and protein concentration was tested using FA. The single phosphorylated peptides were used so that a potential stabilizing effect could be correlated to a specific binding motif. 14-3-3γ was used because of the highest binding affinity of all peptides to this isoform.

The FA results showed that several FCs have a stabilizing effect on the p65_45^{E}/14-3-3γ and p65_45^{R}/14-3-3γ interaction (Figure 3C; Figure S3), while they do not stabilize the p65_281/14-3-3γ complex (Figure S3). The fusicoccanes FC-A, FC-J and FC-NAc elicited about two-fold higher anisotropy signal of the p65_45^{R}/14-3-3γ PPI compared to the DMSO control. Interestingly, semi-synthetic analogues DP-005 and ISIR-005 induced a stronger increase in the anisotropy signal (about three-fold). Bulky extensions at the C-ring (FC-THF) and the absence of the sugar moiety (FC-A-ag and FC-J-ag) abrogated the ability to stabilize the p65_45^{R}/14-3-3γ complex. A hydroxyl group at the 12-position or its ring-extension thus cause a loss in activity. The negligible activity of the aglycons is in line with previous work on these synthetic variants, generally showing lower activity.[42]

The stabilizing effects of FC-A and DP-005 were further investigated via 14-3-3γ protein titrations to the p65_45^{R} peptide at a set concentration of DP-005, FC-A, or the DMSO control (Figure 3D). The protein titrations confirmed the stronger stabilizing effect of DP-005 as compared to FC-A, with a clear left shift

of the binding curve, affording apparent K_D values of 2.8±0.1 μM and 38.9±2.4 μM respectively. Constraining the fitting for the DMSO control, using the upper plateau of the DP-005 and FC-A binding curves, results in an apparent K_D of about 350 μM for the p65_45^R/14-3-3γ complex.

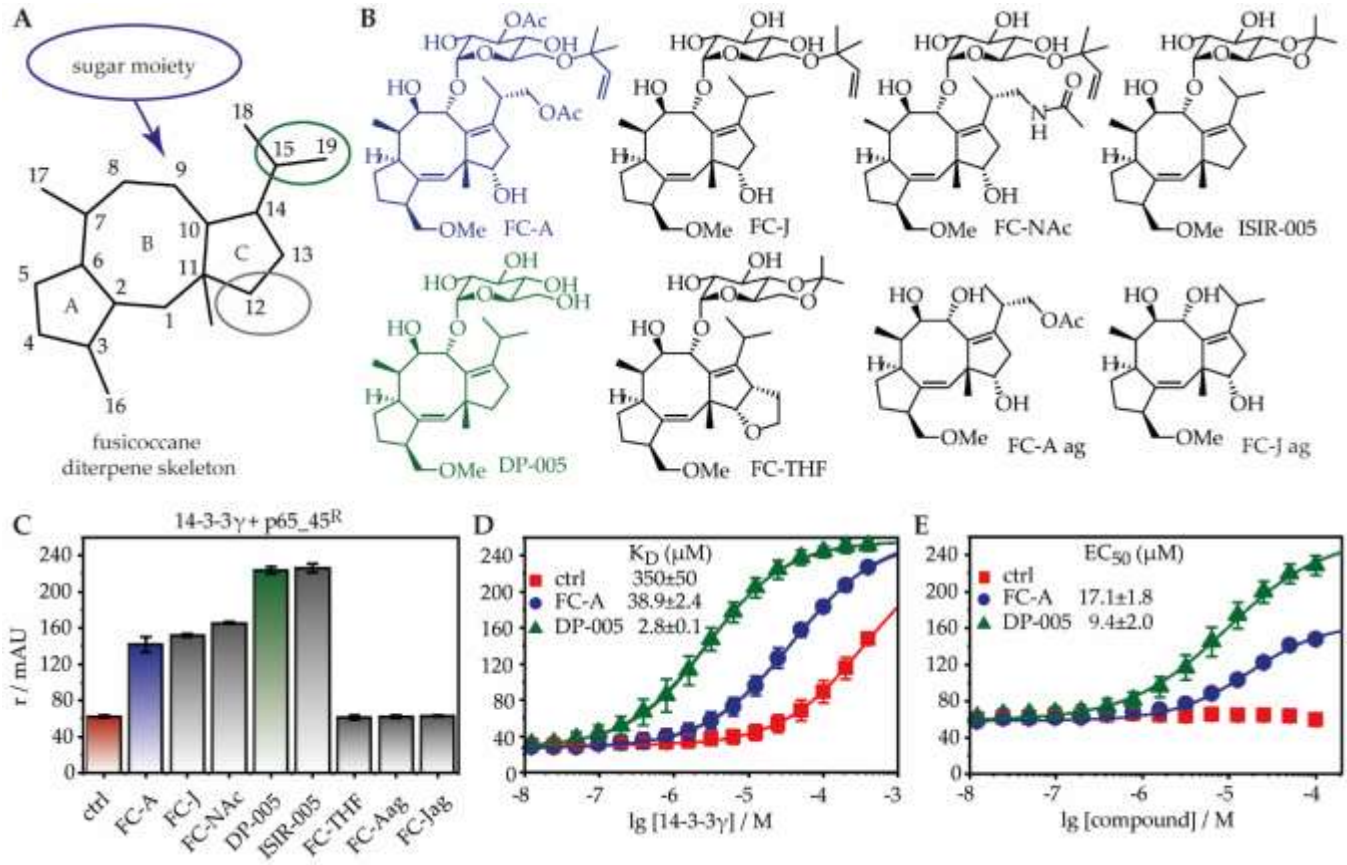

Figure 3: Stabilizing effect of fusicoccanes on the p65_45/14-3-3 interaction. (A) The diterpene skeleton of the fusicoccane family. Encircled are the positions which are of interest in this study. (B) A collection of eight FCs used to screen for a stabilizing effect on the p65/14-3-3 complex. (C) FA-based screening results of the FC-collection shown in B on the p65_45^{R}-14-3-3γ complex. The anisotropy (r in mAU) measurements were carried out with 100 μM compound, 50 μM 14-3-3γ and 100 nM of p65_45^{R}. Error bars represent standard deviations of two independent measurements performed in technical triplicates. (D) Titration of 14-3-3γ in the presence of 100 μM compound or DMSO control (ctrl) and 100 nM p65_45^{R} measured with FA. Error bars represent standard deviations of three independent singlet measurements. (E) Titration of compound or DMSO control (ctrl) in presence of 50 μM 14-3-3γ and 100 nM p65_45^{R} measured with FA. Error bars represent standard deviations of three independent singlet measurements.

Hence, the improvement in peptide stabilization acquaints to approximately 10-fold (FC-A) and 100-fold (DP-005) compared with the DMSO control. Finally, the effective concentrations of FC-A and DP-005 were determined by titrating the compounds to a fixed protein and peptide concentration of 50 μM and 100 nM respectively. This gave an EC_{50} of 9.4±2.0 μM for the semi-synthetic compound DP-005, while the natural compound FC-A showed a weaker activity with an EC_{50} of 17.1±1.8 μM (Figure 3E).

Crystallography and NMR provides structural confirmation of the FC binding to p65/14-3-3. To corroborate the stabilization and SAR obtained using FA, we sought a structural analysis of the ternary complex of DP-005 with p65_45^{R}/14-3-3. For this purpose, DP-005 was soaked into crystals of the pre-formed p65_45^{R}/14-3-3σΔC complexes, revealing extra electron density for the p65_45^{R}/14-3-3σΔC crystals. This electron density allowed for the complete refinement of DP-005 (Figure 4A, Table S1, PDB ID: 6NV2). The crystal structure provided detailed information about the orientation of the diterpenoid

core and the sugar moiety. Of note, the orientation of the peptide changed significantly upon binding of DP-005 (Figure 4B). In particular, amino acid P47 changed from a *trans*- to a *cis*-conformation and the residues from G48 to S51 moved away from the ligand. The most prominent interactions between DP-005 and the protein complex are the hydrophobic contacts with I46 and P47 of p65_45^{R} as well as with L218, I219 and L222 of 14-3-3σΔC (Figure 4C). Noteworthy is the contact of the methoxy group of DP-005 with the ε-amino group of K122 of the protein, while the sugar moiety was surrounded by the water shell of 14-3-3σΔC (Figure 4D). The fact that FC-aglycons showed only a negligible activity, might be due to the importance of this sugar-water shell interaction.

An overlay of FC-A with the conformation of DP-005 points out the impact of the singular hydroxyl group at the 12-position of FC-A, not present in DP-005, on the binding to the protein complex (Figure 4E). The hydroxyl group would have an orientation that would induce a steric and polar clash with hydrophobic elements of the peptide. This indicates that the peptide would potentially require further rearrangements in order to accommodate the binding of FC-A, potentially explaining why the ternary structure of FC-A/p65_45^{R}/14-3-3σΔC could not be determined with X-ray crystallography.

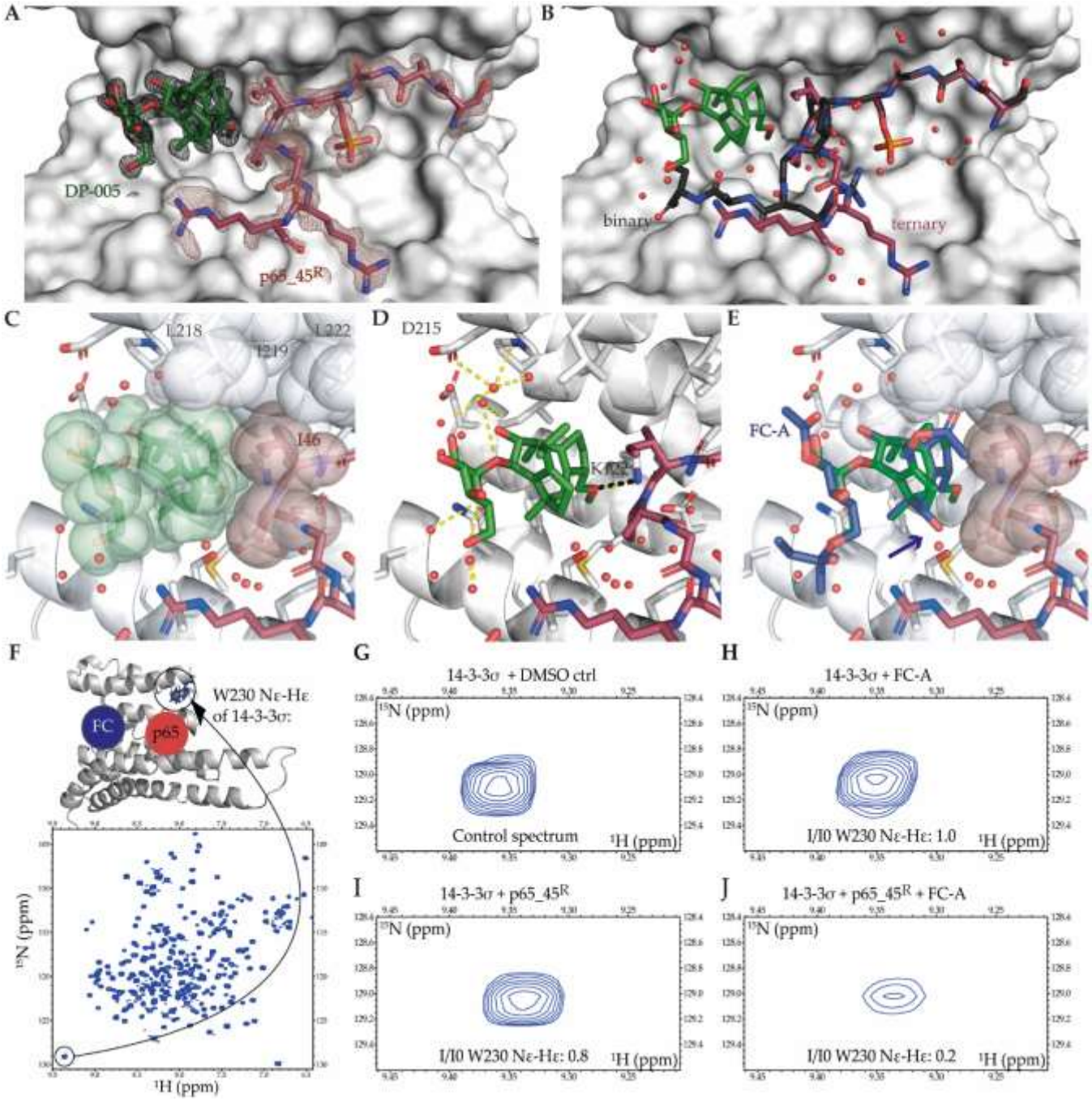

Figure 4: Structural analysis of the ternary DP-005/p65/14-3-3 and FC-A/p65/14-3-3 complexes. (A) Crystal structure of DP-005 (green sticks), p65_45 (red sticks) and 14-3-3σΔC (white surface) (PDB ID: 6NV2). (B) Binding of DP-005 induces a re-orientation of the p65_45 peptide (original conformation of binary complex: black sticks; ternary complex with DP-005: red sticks). (C) Hydrophobic contacts are indicated with spheres. (D) Polar contacts of DP-005 displayed as yellow dashed lines with the polar contact of the methoxy group of DP-005 and K122 highlighted with black dashed lines. (E) Overlay of FC-A (blue sticks) and DP-005 (green sticks). An arrow indicates the hydroxyl group at position 12 which causes the difference in affinity between both compounds. Hydrophobic residues of the peptide/protein complex are shown as spheres. (F) The resonance corresponding to the W230 Nε-Hε bond of 14-3-3σ was monitored to detect the stabilization of this PPI. This resonance is circled in black on the ^{1}H-^{15}N TROSY-HSQC spectrum of $^{15}N^{13}C^{2}H$-labeled 14-3-3σ (shown on the right) and the corresponding residue W230 is represented as sticks, colored in blue and circled in black on the crystal structure (shown on the left, represented as white surface). This residue is close to the peptide-binding site and distant from the FC-A binding site. (G-J) The enlarged spectral region of the 1H-15N TROSY-HSQC containing the resonance corresponding to the W230 Nε-Hε bond of 14-3-3σ (125 µM) is shown in the presence of: DMSO 4% (v/v), present in all samples (G) , FC-A 125 µM (H), p65_45^{R} peptide 625 µM (I) and p65_45^{R} peptide 625 µM and FC-A 125 µM (J).

As an alternative to obtaining structural information on the binding of FC-A to the binary p65/14-3-3 complex, NMR measurements were performed, based on the assignments of 14-3-3σ signals.[43] Chemical shift perturbations in the resonances corresponding to specific residues along 14-3-3σ confirmed that FC-A binds in its previously reported binding pocket, in the presence and in the absence of the p65_45 peptide (Figure S4). To specifically monitor the binding event of p65_45^{R} to 14-3-3σ, we focused on the ^{1}H-^{15}N TROSY-HSQC signature of residue W230 side-chain of $^{15}N^{13}C^{2}H$ labeled 14-3-3σ. This residue is specifically affected by the p65_45^{R} peptide binding, but not by the FC-A binding, as can be expected from its remote position from the FC-A binding pocket (Figure 4F). Its side-chain Nε-Hε resonance has a clear signature because it is isolated in the spectrum (Figure 4F) and is unambiguously assigned (Figure S5). Monitoring the resonance intensity of Nε-Hε W230 revealed that the intensity of this resonance is, as expected, not affected by the presence of FC-A alone (Figure 4G,H). Addition of the p65_45^{R} peptide alone results in resonance broadening due to the binding, and an intensity drop to 80% as compared to the reference spectrum (Figure 4I). Addition of FC-A together with the p65_45 peptide resulted in the most pronounced decrease of the intensity of the Nε-Hε W230 resonance, down to 20% (Figure 4J). The data thus orthogonally confirm the stabilization of the p65_45^{R}/14-3-3σ complex by FC-A.

Preferential stabilization of the p65/14-3-3 complex by DP-005. The stabilization of p65/14-3-3 by DP-005 was significantly stronger than the effect of FC-A (*vide supra*), raising the question about DP-005 impact on other FC responsive 14-3-3 PPIs. Crucial differences between FC-A and DP-005 are the additional polar decorations of FC-A at positions 12 and 19 (Figure 3 A,B). Hence, we hypothesized based on the crystal structure of the ternary complex that the hydrophobic contacts of the Ile and Pro at the +1 and +2 positions of the p65_45^{R} peptide match the complementary driving force of the DP-005 based stabilization. Within the FC responsive 14-3-3 PPIs, diverse amino acid sequences C-terminal from the phosphorylation site, can be found.[18–22] We investigated the effects of FC-A and DP-005 on a small set of three different clinically relevant 14-3-3 interaction partners (CFTR,[44,45] c-Raf[35,46] and p53[47,48]) which differ in size and hydrophobicity of the +1 amino acid (Figure 5A).

CFTR binds to 14-3-3 via multiple phosphorylation sites, for which the combination of two, pS753 and pS768 (CFTR_bi), was suggested to give a suitable representation of the biological situation.[22] Both binding sites host a valine at the +1 and an isoleucine or leucine at the +2 position and they bind in an elongated manner within the 14-3-3 binding groove (Figure 5A, Figure S6A,B). Upon binding of FC-A only the pS753 site is flexible enough to rearrange allowing the formation of a ternary complex (Figure 5B, Figure

S6C). FA assays with the single phosphorylated peptides, representing the two binding sites, confirm that only the pS753 site is responsive to FC-A or DP-005 (Figure S6A,B).

The example of CFTR is particularly interesting since the binding behavior of the CFTR peptides show similarities with the p65 peptides: for both interactions a bivalent binding mode is suggested and only one of the two binding sites is responsive to FCs. Therefore, the bivalent p65_bi^R and CFTR_bi peptides were used to measure the effects of FC-A and DP-005 on complex formation with 14-3-3γ. While FC-A and DP-005 have the same stabilizing effect on the bivalent CFTR_bi/14-3-3γ PPI, DP-005 has a 10x stronger stabilizing effect than FC-A on the p65_bi^R/14-3-3γ complex (Figure 5 C-E). The relative shift in apparent K_D induced by the FCs are the same for the monovalent p65_45^R and the bivalent p65_bi^R (Figure 3D, Figure 5D,E), showing that the increased binding affinity of the bivalent peptide does not change the stabilizing effects of FCs on the binding site pS45 of p65. Also, DP-005 is more active on the p65/14-3-3γ than the CFTR/14-3-3γ complex, although the CFTR_753 peptide offers a similar hydrophobic environment as the p65_45^R peptide. Based on the crystal structures, it can be hypothesized that the +2 position is crucial for this difference. Due to the alternating orientations of the amino acid side chains of unstructured motifs the isoleucine at the +2 position of the CFTR_753 is pointing towards the phosphorylated residue (Figure S6). In this orientation the Ile is not able to establish favorable hydrophobic contacts with DP-005, unlike the proline at the +2 position of the p65_45 peptide (Fig. 4C).

For c-Raf two 14-3-3 binding sites are reported, pS233 and pS259, which both host a more polar threonine at the +1 and a proline at the +2 positions (Figure 5A).[19] This interaction is not stabilized by FC-A[11], therefore it was interesting to analyze the stabilization achievable with DP-005 on the c-Raf_259/14-3-3 complex. In the presence of DP-005 the c-Raf_259 peptide binds 2x stronger to 14-3-3γ, while the lack of stabilization for FC-A could be reproduced (Figure 5C-E). This shows that a small polar amino acid at the +1 position reduces the stabilizing effect of DP-005, confirming that mostly hydrophobic contacts between this FC derivative, the peptide and 14-3-3 are necessary to establish the cooperative binding.

p53 binds to 14-3-3 via its C-terminal domain and one of multiple possible phosphorylated binding sites. The pT387 site, was co-crystallized with 14-3-3,[47–49] the binding sequence is bound in a bent conformation to the 14-3-3 binding groove and it hosts a large, polar glutamic acid at the +1 position (Figure 5A,B). The bent motif should allow FCs to bind, but crystal structures of the ternary FC-A/p53/14-3-3σΔC complex showed that the electron density for the peptide is not resolved in the presence of FC-A.[18] Still, FC-A shows a stabilization of the p53/14-3-3 interaction by reducing the apparent K_D by a factor of 2, whereas DP-005 has no significant effect on the p53/14-3-3 complex (Figure 5C-E). DP-005 thus has a specific and very strong stabilization effect on the p65 sequence exclusively.

Cooperativity Factor as a Measure of Concentration Independent Stabilization. The relative effect of a set FC concentration on the examined 14-3-3 PPIs revealed major differences in stabilization potency. These measurements were performed at a single, fairly high concentration of FCs and give no information about the effective range of FC concentrations, the concentrations needed to reach saturation of the system or the low threshold concentration necessary to achieve stabilization. Cooperativity analysis was done in order to gain a deeper understanding of relevant concentrations and to quantify the preferential stabilization of p65 by DP-005, over other targets via the concentration independent cooperativity factor α (Figure S7, Table S2). The α-factor describes the enhancement of binding affinity of a ternary complex formation compared to a binary complex.[9,11,12] To calculate this factor, 14-3-3γ titrations were performed in the presence of a variety of constant concentrations of DP-005 or FC-A stabilizer on the p65, CFTR, c-Raf, and p53/14-3-3 interactions (Figure 6A,B, Figure S8,S9). The highest FC concentration used was 250 μM which was reduced stepwise in a 1:2 dilution series. At increasing concentrations of compound, the protein has an increasing partial occupancy of bound stabilizer during the titrations. Due to cooperative binding this leads to more peptide binding at lower protein concentrations, hence a left shift of the binding curves resulting in a 2D stabilizing-profile.[11]

For FC-A the apparent K_D's of the p65_bi^R and CFTR_bi in complex with 14-3-3γ shift an order of magnitude from about 10 μM to 1 μM for both peptides (Figure 6A). Increasing concentrations of FC-A also induce a shift in the upper plateau, most likely due to a tighter binding peptide. Unlike FC-A, DP-005 induces about a 100-fold decrease of apparent K_D-values for the p65_bi^R/14-3-3γ complex, while the curves for the DP-005/CFTR_bi/14-3-3γ complexes are comparable to the curves for FC-A with a shift of only one order of magnitude (Figure 6B). DP-005 also causes an increase of anisotropy values for the upper plateau. These data were fitted using the Hill equation and the resulting apparent K_D's in presence of the FCs (K_D^{app}) were divided by the K_D of the binary complex (K_D^I). It is expected that at a certain stabilizer concentration the system is saturated, resulting in no further reduction of apparent K_D-values with increasing concentrations of stabilizer. This saturated system can be used to extrapolate the cooperativity factor α (Figure 6C, Table S2). This value represents the maximum reduction of K_D induced via the stabilizer and can be derived from the ratio of the dissociation constant of the binary complex and the apparent K_D of the complex saturated with stabilizer (more information see SI). By plotting the K_D^I/K_D^{app} ratio versus the FC concentration not only the α-factor, but also a threshold concentration can be extracted (Figure 6D,E). This concentration is the minimal required FC concentration needed to induce cooperative formation of the ternary complex. The threshold concentration of FC-A was 10 μM for both the p65_bi^R and CFTR_bi (Figure 6D,E). The FC-A/p65/14-3-3γ complex reached saturation with 30 μM FC-A, as

higher concentrations do not change the ratio of K_D^I/K_D^{app} anymore (Figure 6D). At the point of saturation, the K_D^I/K_D^{app} gives an α-value of 5 for the FC-A/p65/14-3-3γ, while for the FC-A/ CFTR_bi/14-3-3γ an α-value of 8 is reached. An α-value of 10 was determined for the DP-005/CFTR_bi/14-3-3γ complex, also with the threshold concentration of 10 μM to induce cooperative binding. In contrast, only 1 μM of DP-005 is needed to induce cooperativity of the DP-005/p65/14-3-3γ complex with an α-value of 120; at least 10x higher than any other measured α-value. DP-005 revealed only a small enhancement of apparent K_D values for c-Raf and p53, even at the highest concentrations. The higher concentrations of FC-A led to a further decrease of K_D^{app} and resulted in an α-value of 3 for the FC-A/p53/14-3-3γ complex. In contrast, the destabilizing effect of FC-A on the c-Raf/14-3-3γ complex becomes more obvious at higher concentrations, while the higher concentrations of DP-005 did not further decrease the K_D^{app}. An α-value of about 1.5 was determined for the DP-005/c-Raf/14-3-3γ and the DP-005/p53/14-3-3γ complex.

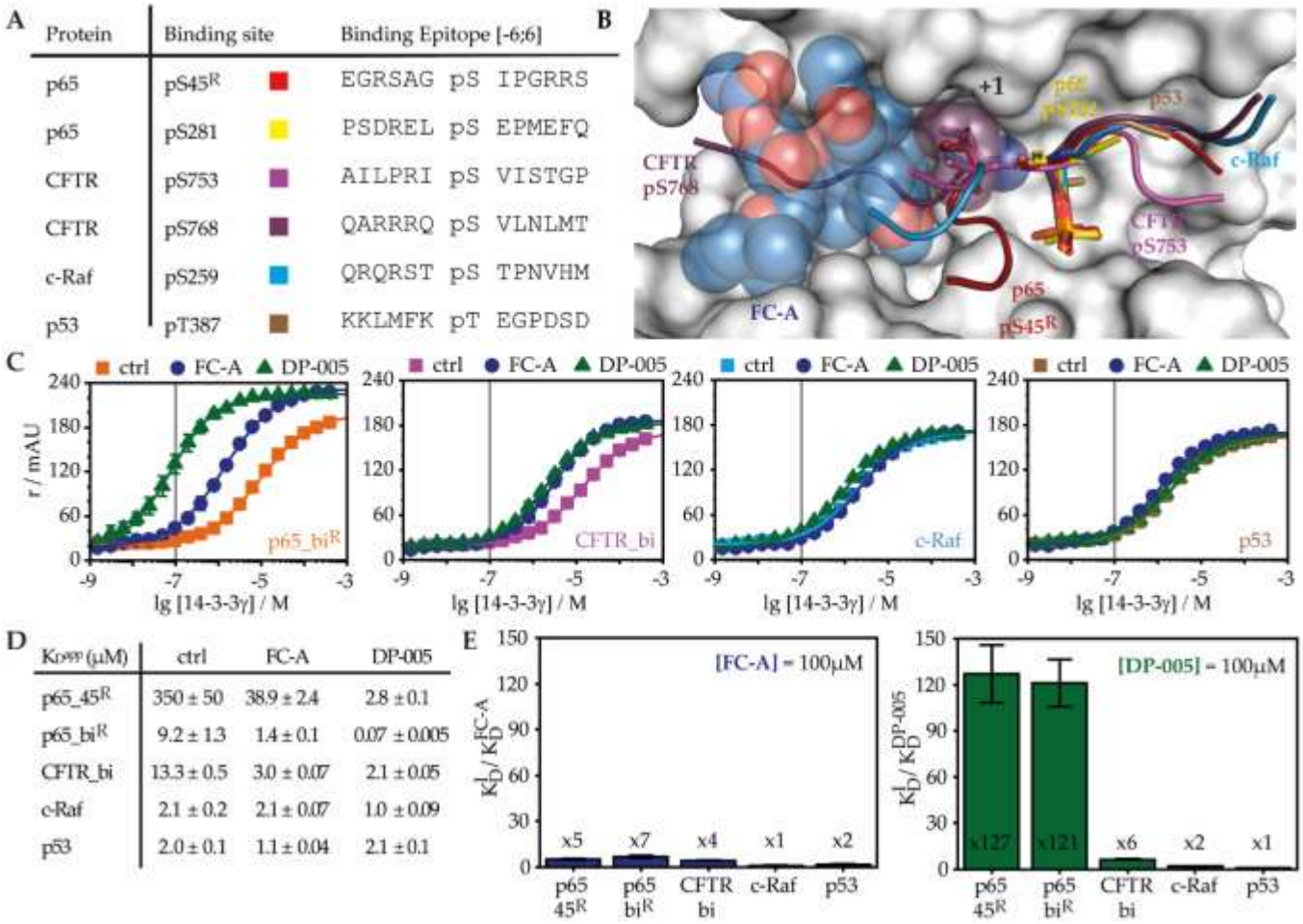

Figure 5: Comparison of FC induced stabilization on 14-3-3 PPIs. (A) Overview of 14-3-3 binding epitopes. (B) Overlay of the crystal structures of the binding epitopes shown in A (cartoon representation, phosphorylated residue and +1 amino acid shown as sticks). FC-A is shown as transparent spheres, 14-3-3 as white van der Waals surface. (C) Binding affinities of indicated peptides were measured for 14-3-3γ in the presence of DMSO as control (ctrl), 100 μM FC-A or 100 μM DP-005 with FA (r in mAU). For peptide sequences see Table 1 and S3). (D) K_D^{app} values in μM for the indicated peptides for the DMSO control (ctrl) or with FC-A or DP-005. (E) Increase in affinity of the binding partners due to FC-A or DP-005 shown as the ratio of the dissociation constant of the DMSO control (K_D^l) divided by the dissociation constant in the presence of either FC-A ($K_D^{FC\text{-}A}$) or DP-005 ($K_D^{DP\text{-}005}$). The numbers indicate the factor with which the binding affinity is enhanced due to the FCs compared to the control.

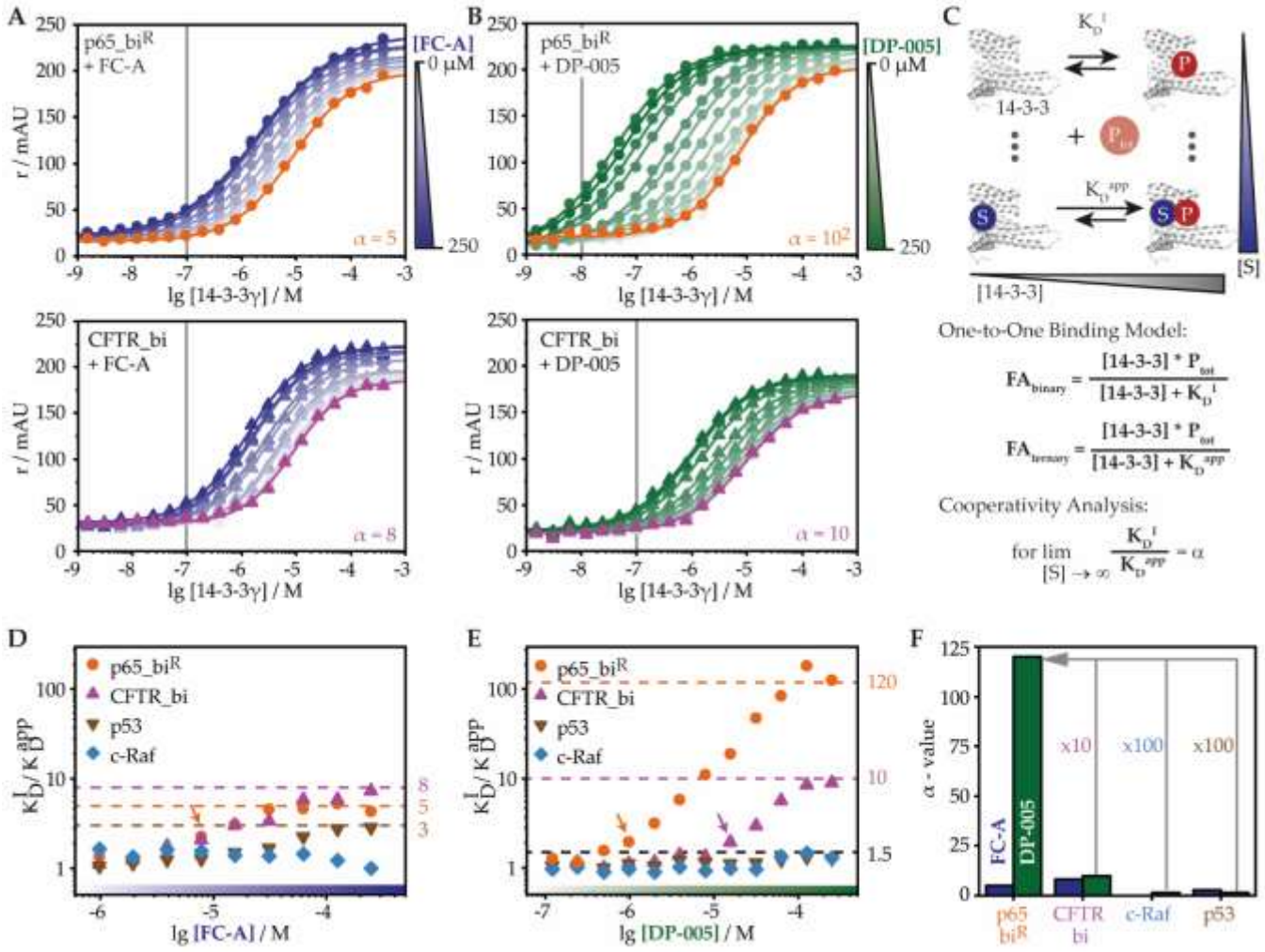

Figure 6: Cooperativity Analysis of FC-A and DP-005 on 14-3-3 PPIs. (A) 2D FA-results of FC-A with p65_bi^R/14-3-3γ and CFTR_bi (n=1). FC-A concentrations ranging from 0-250 µM, the vertical grey line indicates the peptide concentration. Anisotropy (r) given in mAU. (B) 2D FA-results of DP-005 with p65_bi^R/14-3-3γ or CFTR_bi (n=1). DP-005 concentrations ranging from 0-250 µM, the vertical grey line indicates the peptide concentration. (C) Scheme of 2D Titration in FA. 14-3-3 was titrated against 100nM of peptide (P) varying fixed concentrations of stabilizer (S). The data analysis was based on a one-to-one binding model. For cooperativity analysis the ratio of K_D of the binary (K_D^I) and ternary (K_D^{app}) complex was used to derive the cooperativity factor α (for derivation of the equations and additional information see SI). (D) K_D^I/K_D^{app} ratio plotted against FC-A concentration for 2D titrations shown in A and Figure S8. The arrow is indicating the minimal active concentration of the stabilizer, while the curve reaches saturation at the α-value. (E) K_D^I/K_D^{app} ratio plotted against DP-005 concentration for 2D titrations shown in B and Figure S9. Analysis is in accordance with D. (F) The cooperativity value α for the ternary complexes with 14-3-3γ and either FC-A or DP-005 was plotted against the different target peptides. DP-005 has a 10-fold stronger effect on the p65/14-3-3γ interaction than any other measured interaction.

CONCLUSIONS

The NF-κB transcriptional pathway plays an essential role in immune response and its deregulation leads to cancer promotion. Targeting this pathway is an unsolved challenge in drug development. A recent review concluded that the intense cross-talk of the numerous signaling pathways acting on the NF-κB transcription factors as well as the only partly understood interplay of the different NF-κB subunits are responsible for the reoccurring failures during clinical trials despite the promising biological studies.[32] A

more focused approach to target specific subunits of NF-κB was suggested. PPI stabilization of p65, a subunit of NF-κB, and 14-3-3 may provide such an opportunity to target NF-κB activity in a subunit specific manner. The interaction of p65 with 14-3-3 is associated with reduced tumor growth in mouse models and recovery after Ischemia-Reperfusion,[24–26] validating this interaction for PPI stabilization studies. Yet, a better fundamental understanding of this interaction in the context of the NF-κB pathway is needed, particularly with regard to translational drug discovery. A stabilizer for the p65/14-3-3 interaction would serve as a tool compound to decipher this pathway and provides a chemical entry point for drug design. The results presented in this manuscript bring the p65/14-3-3 complex forward as an excellent candidate for PPI stabilization, specifically due to the orientation of the p65_45^{R} peptide within the 14-3-3 binding groove, creating a well-defined interface pocket that could be stabilized with FC-based natural products.

Natural compounds provide for unique tools to probe and interrogate unique regions of chemical space,[50] which can be extended and brought to higher levels of control and specificity through their chemical modifications.[23] A number of 14-3-3-based PPIs are stabilized by FCs with correlated positive effects on the underlying biological systems, such as tumor growth reduction by Cotylenin A[19] or improved neural regeneration with FC-A[51]. While DP-005 is generally a weaker stabilizer than FC-A for 14-3-3 PPIs, here we revealed that, in contrast, DP-005 has the strongest stabilizing capability of all FCs for the p65/14-3-3 interaction, being 10-fold more potent than FC-A. The structural elucidation of the DP-005 binding mode identified the key elements required for highly cooperative binding, including specific hydrophobic contacts with the p65 partner epitope and 14-3-3 K122 as a polar anchor.

Cooperativity analysis has been shown to be a powerful tool to explain and compare the efficacy of PPI stabilizers and to optimize their affinity.[11,12] The high cooperativity of DP-005 for stabilizing the p65/14-3-3 interaction highlights that a relatively small modification to a small-molecule PPI stabilizer can have profound effects on the magnitude of the cooperativity. Specifically, the results revealed a strong increase in PPI selectivity by virtue of this cooperativity. The non-differentiated stabilizing effects of FC-A, FC-J and FC-NAc on the p65/14-3-3 complex demonstrate that a higher intrinsic affinity of the stabilizer (FC-A and FC-J have similar binding affinities towards 14-3-3, while FC-NAc has a significantly higher affinity[11,23]) does not necessarily translate into better PPI stabilization. The higher cooperativity of DP-005 for the p65/14-3-3 PPI resulted in its most favorable stabilization, while simultaneously featuring a similar or weaker capacity to stabilize other 14-3-3 PPIs, thus leading to selectivity. High potency and selectivity are needed in drug discovery to allow low doses of compound to be used but also to minimize off-target

effects. Cooperativity analysis as described here represents an excellent approach to define the concentration regime under which a stabilizer might be useful and identify compounds likely to elicit good selectivity early in the drug discovery process.

In conclusion, this study provides the structural and biophysical basis of the p65/14-3-3 interaction as an important step in the identification and rational design of small-molecule modulators. Specifically the FC natural products and derivatives are shown to be highly promising tool compounds, with chemical entries to achieving PPI selective stabilization, by means of cooperativity. The high cooperativity of the most promising compound DP-005 also results in a low threshold concentration for realizing PPI-stabilization. This study highlights the way towards selective PPI stabilization, with cooperativity analysis providing an analytical tool to guide compound or stabilizer optimization in PPI drug discovery projects.

ASSOCIATED CONTENT

p65 sequence homology, detailed fluorescence anisotropy data, peptide sequences, protein expression and purification, crystallography details, extensive clarification of the mass balance model, materials and methods including compound synthesis and characterization, are available in the Electronic Supplementary Information (ESI).

AUTHOR INFORMATION

Corresponding Author

* Correspondence: c.ottmann@tue.nl

Author Contributions

The manuscript was written through contributions of all authors. All authors have given approval to the final version of the manuscript.

Funding Sources

The research is supported by funding from the European Union through the TASPPI project (H2020-MSCA-ITN-2015, grant number 675179) and by the LabEx (Laboratory of Excellence) DISTALZ (ANR, ANR-11-LABX- 009) and through The Netherlands Organization for Scientific Research (NWO) via VICI grant 016.150.366 and via Gravity Program 024.001.035. The NMR facilities were funded by the Nord Region Council, CNRS, Institut Pasteur de Lille, the European Community (ERDF), the French Ministry of Research and the University of Lille. We acknowledge support for the NMR facilities from

TGE RMN THC (CNRS, FR-3050) and FRABio (Univ. Lille, CNRS, FR-3688). This work was supported by the EPSRC (EP/N013573/1), and The Wellcome Trust (097827/Z/11/A).

ACKNOWLEDGMENT

We thank François-Xavier Cantrelle from the University of Lille for NMR data acquisition.

ABBREVIATIONS

PPI, protein protein interaction; CFTR, Cystic fibrosis transmembrane conductance regulator; c-Raf, RAF proto-oncogene serine/threonine-protein kinase; DP-005, semi-synthetic natural compound; EC50, Half maximal effective concentration; ERα, Estrogen receptor alpha; FA, fluorescence anisotropy; FC, fusicoccane class of natural compounds; FC-A, natural compound; Gab2, GRB2-associated-binding protein 2; IC50, Half maximal inhibitory concentration; IκBα, NF-κB inhibitor alpha; K_D, Dissociation constant; NF-κB, nuclear factor kappa-light-chain-enhancer of activated B cells; p53, Tumor protein p53; PROTACS, proteolysis-targeting chimeras; p65, RelA subunit of NF-κB; r, anisotropy; SAR, structure activity relationship; TNFα, Tumour Necrosis Factor alpha.

REFERENCES

(1) Wells, J. A., and McClendon, C. L. (2007) Reaching for high-hanging fruit in drug discovery at protein–protein interfaces. *Nature 450*, 1001–1009.

(2) Scott, D. E., Bayly, A. R., Abell, C., and Skidmore, J. (2016) Small molecules, big targets: drug discovery faces the protein–protein interaction challenge. *Nat. Rev. Drug Discov. 15*, 533–550.

(3) Andrei, S. A., Sijbesma, E., Hann, M., Davis, J., O'Mahony, G., Perry, M. W. D., Karawajczyk, A., Eickhoff, J., Brunsveld, L., Doveston, R. G., Milroy, L.-G., and Ottmann, C. (2017) Stabilization of protein-protein interactions in drug discovery. *Expert Opin. Drug Discov. 12*, 925–940.

(4) Cochran, A. G., Conery, A. R., and Sims, R. J. (2019) Bromodomains: a new target class for drug development. *Nat. Rev. Drug Discov. 18*, 609–628.

(5) Stevers, L. M., Sijbesma, E., Botta, M., MacKintosh, C., Obsil, T., Landrieu, I., Cau, Y., Wilson, A. J., Karawajczyk, A., Eickhoff, J., Davis, J., Hann, M., O'Mahony, G., Doveston, R. G., Brunsveld, L., and Ottmann, C. (2017) Modulators of 14-3-3 Protein–Protein Interactions. *J. Med. Chem. 61*, 3755–3778.

(6) Fischer, E. S., Park, E., Eck, M. J., and Thomä, N. H. (2016) SPLINTS: small-molecule protein ligand interface stabilizers. *Curr. Opin. Struct. Biol. 37*, 115–122.

(7) Milroy, L.-G., Grossmann, T. N., Hennig, S., Brunsveld, L., and Ottmann, C. (2014) Modulators of Protein–Protein Interactions. *Chem. Rev. 114*, 4695–4748.

(8) Whitty, A. (2008) Cooperativity and biological complexity. *Nat. Chem. Biol. 4*, 435–439.

(9) Ehlert, F. J. (1988) Estimation of the affinities of allosteric ligands using radioligand binding and pharmacological null methods. *Mol. Pharmacol. 33*, 187–194.

(10) Williamson, J. R. (2008) Cooperativity in macromolecular assembly. *Nat. Chem. Biol. 4*, 458–465.

(11) Vink, P. J. de, Andrei, S. A., Higuchi, Y., Ottmann, C., Milroy, L.-G., and Brunsveld, L. (2019) Cooperativity basis for small-molecule stabilization of protein–protein interactions. *Chem. Sci. 10*, 2869–2874.

(12) Gadd, M. S., Testa, A., Lucas, X., Chan, K.-H., Chen, W., Lamont, D. J., Zengerle, M., and Ciulli, A. (2017) Structural basis of PROTAC cooperative recognition for selective protein degradation. *Nat. Chem. Biol. 13*, 514–521.

(13) Flynn, D. C. (2001) Adaptor proteins. *Oncogene 20*, 6270–6272.

(14) Aghazadeh, Y., and Papadopoulos, V. (2016) The role of the 14-3-3 protein family in health, disease, and drug development. *Drug Discov. Today 21*, 278–287.

(15) Aitken, A. (2006) 14-3-3 proteins: A historic overview. *Semin. Cancer Biol. 16*, 162–172.

(16) Stevers, L. M., de Vink, P. J., Ottmann, C., Huskens, J., and Brunsveld, L. (2018) A Thermodynamic Model for Multivalency in 14-3-3 Protein–Protein Interactions. *J. Am. Chem. Soc. 140*, 14498–14510.

(17) Obsil, T., and Obsilova, V. (2011) Structural basis of 14-3-3 protein functions. *Semin. Cell Dev. Biol. 22*, 663–672.

(18) Doveston, R. G., Kuusk, A., Andrei, S., Leysen, S., Cao, Q., Castaldi, P., Hendricks, A., Chen, H., Boyd, H., and Ottmann, C. Small-Molecule Stabilization of the p53 – 14-3-3 Protein-Protein Interaction. *FEBS Lett. 591*, 2449–2457.

(19) Molzan, M., Kasper, S., Röglin, L., Skwarczynska, M., Sassa, T., Inoue, T., Breitenbuecher, F., Ohkanda, J., Kato, N., Schuler, M., and Ottmann, C. (2013) Stabilization of Physical RAF/14-3-3 Interaction by Cotylenin A as Treatment Strategy for RAS Mutant Cancers. *ACS Chem. Biol. 8*, 1869–1875.

(20) De Vries-van Leeuwen, I. J., da Costa Pereira, D., Flach, K. D., Piersma, S. R., Haase, C., Bier, D., Yalcin, Z., Michalides, R., Feenstra, K. A., Jimenez, C. R., de Greef, T. F. A., Brunsveld, L., Ottmann, C.,

Zwart, W., and de Boer, A. H. (2013) Interaction of 14-3-3 proteins with the Estrogen Receptor Alpha F domain provides a drug target interface. *Proc. Natl. Acad. Sci. 110*, 8894–8899.

(21) Bier, D., Bartel, M., Sies, K., Halbach, S., Higuchi, Y., Haranosono, Y., Brummer, T., Kato, N., and Ottmann, C. (2016) Small-Molecule Stabilization of the 14-3-3/Gab2 Protein–Protein Interaction (PPI) Interface. *ChemMedChem 11*, 911–918.

(22) Stevers, L. M., Lam, C. V., Leysen, S. F. R., Meijer, F. A., van Scheppingen, D. S., de Vries, R. M. J. M., Carlile, G. W., Milroy, L. G., Thomas, D. Y., Brunsveld, L., and Ottmann, C. (2016) Characterization and small-molecule stabilization of the multisite tandem binding between 14-3-3 and the R domain of CFTR. *Proc. Natl. Acad. Sci. U. S. A. 113*, E1152-1161.

(23) Andrei, S. A., de Vink, P., Sijbesma, E., Han, L., Brunsveld, L., Kato, N., Ottmann, C., and Higuchi, Y. (2018) Rationally Designed Semisynthetic Natural Product Analogues for Stabilization of 14-3-3 Protein–Protein Interactions. *Angew. Chem. Int. Ed. 57*, 13470–13474.

(24) Aguilera, C., Fernández-Majada, V., Inglés-Esteve, J., Rodilla, V., Bigas, A., and Espinosa, L. (2006) Efficient nuclear export of p65-IκBα complexes requires 14-3-3 proteins. *J. Cell Sci. 129*, 2472–2472.

(25) Inglés-Esteve, J., Morales, M., Dalmases, A., Garcia-Carbonell, R., Jené-Sanz, A., López-Bigas, N., Iglesias, M., Ruiz-Herguido, C., Rovira, A., Rojo, F., Albanell, J., Gomis, R. R., Bigas, A., and Espinosa, L. (2012) Inhibition of Specific NF-κB Activity Contributes to the Tumor Suppressor Function of 14-3-3σ in Breast Cancer. *PLoS ONE 7*, e38347.

(26) Zhou, X., Hu, D. X., Chen, R. Q., Chen, X. Q., Dong, W., and Yi, C. (2017) 14-3-3 Isoforms Differentially Regulate NFκB Signaling in the Brain After Ischemia-Reperfusion. *Neurochem. Res. 42*, 2354–2362.

(27) Li, Q., and Verma, I. M. (2002) NF-κB regulation in the immune system. *Nat. Rev. Immunol. 2*, 725–734.

(28) Nakanishi, C., and Toi, M. (2005) Nuclear factor-κB inhibitors as sensitizers to anticancer drugs. *Nat. Rev. Cancer 5*, 297–309.

(29) Taniguchi, K., and Karin, M. (2018) NF-κB, inflammation, immunity and cancer: coming of age. *Nat. Rev. Immunol. 18*, 309–324.

(30) Arepalli, S. K., Choi, M., Jung, J.-K., and Lee, H. (2015) Novel NF-κB inhibitors: a patent review (2011 – 2014). *Expert Opin. Ther. Pat. 25*, 319–334.

(31) Paul, A., Edwards, J., Pepper, C., and Mackay, S. (2018) Inhibitory-κB Kinase (IKK) α and Nuclear Factor-κB (NFκB)-Inducing Kinase (NIK) as Anti-Cancer Drug Targets. *Cells 7*, E176.

(32) Kaltschmidt, B., Greiner, J., Kadhim, H., Kaltschmidt, C., Kaltschmidt, B., Greiner, J. F. W., Kadhim, H. M., and Kaltschmidt, C. (2018) Subunit-Specific Role of NF-κB in Cancer. *Biomedicines 6*, 44.

(33) Lanucara, F., Lam, C., Mann, J., Monie, T. P., Colombo, S. A. P., Holman, S. W., Boyd, J., Dange, M. C., Mann, D. A., White, M. R. H., and Eyers, C. E. (2016) Dynamic phosphorylation of RelA on Ser42 and Ser45 in response to TNFα stimulation regulates DNA binding and transcription. *Open Biol. 6*, 160055.

(34) Stevers, L., Vries, R. de, Doveston, R., Milroy, L.-G., Brunsveld, L., and Ottmann, C. (2017) Structural interface between LRRK2 and 14-3-3 protein. *Biochem. J. 474*, 1273–1287.

(35) Molzan, M., and Ottmann, C. (2012) Synergistic Binding of the Phosphorylated S233- and S259-Binding Sites of C-RAF to One 14-3-3ζ Dimer. *J. Mol. Biol. 423*, 486–495.

(36) Deloukas, P., and Loon, A. P. G. M. van. (1993) Genomic organization of the gene encoding the p65 subunit of NF-xB: multiple variants of the p65 protein may be generated by alternative splicing. *Hum. Mol. Genet. 2*, 1895–1900.

(37) Ballone, A., Centorrino, F., Wolter, M., and Ottmann, C. (2018) Structural characterization of 14-3-3ζ in complex with the human Son of sevenless homolog 1 (SOS1). *J. Struct. Biol. 202*, 210–215.

(38) Centorrino, F., Ballone, A., Wolter, M., and Ottmann, C. (2018) Biophysical and structural insight into the USP8/14-3-3 interaction. *FEBS Lett. 592*, 1211–1220.

(39) Kuwata, K., Hanaya, K., Higashibayashi, S., Sugai, T., and Shoji, M. (2017) Synthesis of the 1,2-seco fusicoccane diterpene skeleton by Stille coupling reaction between the highly functionalized A and C ring segments of cotylenin A. *Tetrahedron 73*, 6039–6045.

(40) de Boer, A. H., and de Vries-van Leeuwen, I. J. (2012) Fusicoccanes: diterpenes with surprising biological functions. *Trends Plant Sci. 17*, 360–368.

(41) Inoue, T., Higuchi, Y., Yoneyama, T., Lin, B., Nunomura, K., Honma, Y., and Kato, N. (2018) Semisynthesis and biological evaluation of a cotylenin A mimic derived from fusicoccin A. *Bioorg. Med. Chem. Lett. 28*, 646–650.

(42) Anders, C., Higuchi, Y., Koschinsky, K., Bartel, M., Schumacher, B., Thiel, P., Nitta, H., Preisig-Müller, R., Schlichthörl, G., Renigunta, V., Ohkanda, J., Daut, J., Kato, N., and Ottmann, C. (2013) A

semisynthetic fusicoccane stabilizes a protein-protein interaction and enhances the expression of K+ channels at the cell surface. *Chem. Biol. 20*, 583–593.

(43) Neves, J. F., Landrieu, I., Merzougui, H., Boll, E., Hanoulle, X., and Cantrelle, F.-X. (2018) Backbone chemical shift assignments of human 14-3-3σ. *Biomol. NMR Assign. 13*, 103–107.

(44) Liang, X., Da Paula, A. C., Bozóky, Z., Zhang, H., Bertrand, C. A., Peters, K. W., Forman-Kay, J. D., and Frizzell, R. A. (2012) Phosphorylation-dependent 14-3-3 protein interactions regulate CFTR biogenesis. *Mol. Biol. Cell 23*, 996–1009.

(45) Bozoky, Z., Krzeminski, M., Muhandiram, R., Birtley, J. R., Al-Zahrani, A., Thomas, P. J., Frizzell, R. A., Ford, R. C., and Forman-Kay, J. D. (2013) Regulatory R region of the CFTR chloride channel is a dynamic integrator of phospho-dependent intra- and intermolecular interactions. *Proc. Natl. Acad. Sci. 110*, E4427–E4436.

(46) Dumaz, N., and Marais, R. (2003) Protein Kinase A Blocks Raf-1 Activity by Stimulating 14-3-3 Binding and Blocking Raf-1 Interaction with Ras. *J. Biol. Chem. 278*, 29819–29823.

(47) Schumacher, B., Mondry, J., Thiel, P., Weyand, M., and Ottmann, C. (2010) Structure of the p53 C-terminus bound to 14-3-3: Implications for stabilization of the p53 tetramer. *FEBS Lett. 584*, 1443–1448.

(48) Rajagopalan, S., Jaulent, A. M., Wells, M., Veprintsev, D. B., and Fersht, A. R. (2008) 14-3-3 activation of DNA binding of p53 by enhancing its association into tetramers. *Nucleic Acids Res. 36*, 5983–5991.

(49) Rajagopalan, S., Sade, R. S., Townsley, F. M., and Fersht, A. R. (2010) Mechanistic differences in the transcriptional activation of p53 by 14-3-3 isoforms. *Nucleic Acids Res. 38*, 893–906.

(50) Rizzo, S., and Waldmann, H. (2014) Development of a Natural-Product-Derived Chemical Toolbox for Modulation of Protein Function. *Chem. Rev. 114*, 4621–4639.

(51) Kaplan, A., Morquette, B., Kroner, A., Leong, S., Madwar, C., Sanz, R., Banerjee, S. L., Antel, J., Bisson, N., David, S., and Fournier, A. E. (2017) Small-Molecule Stabilization of 14-3-3 Protein-Protein Interactions Stimulates Axon Regeneration. *Neuron 93*, 1082-1093.e5.